

Rapid adjustment of shoreline behavior to changing seasonality of storms: observations and modelling at an open-coast beach

Kristen D. Splinter,^{1*} Ian L. Turner,¹ Mika Reinhardt¹ and Gerben Ruessink²

¹ Water Research Laboratory, School of Civil and Environmental Engineering, UNSW Australia, Sydney, Australia

² Department of Physical Geography, Faculty of Geosciences, Utrecht University, The Netherlands

Received 28 October 2015; Revised 7 November 2016; Accepted 17 November 2016

*Correspondence to: Kristen D. Splinter, Water Research Laboratory, School of Civil and Environmental Engineering, UNSW Australia, Sydney, Australia.

E-mail: k.splinter@unsw.edu.au

ESPL

Earth Surface Processes and Landforms

ABSTRACT: An 8-year time series of weekly shoreline data collected at the Gold Coast, Australia, is used to examine the temporal evolution of a beach, focusing on the frequency response of the shoreline to time-varying wave height and period. Intriguingly, during 2005 the movement of the shoreline at this site changed from a seasonally-dominated mode (annual cycle) to a storm-dominated (~monthly) mode. This unexpected observation provides the opportunity to explore the drivers of the observed shoreline response. Utilizing the calibration of an equilibrium shoreline model to explore the time-scales of underlying beach behavior, the best-fit frequency response (days^{-1}) is shown to be an order of magnitude higher post-2004, suggesting that a relatively subtle change in wave forcing can drive a significant change in shoreline response. Analysis of available wave data reveals a statistically significant change in the seasonality of storms, from predominantly occurring at the start of the year pre-2005 to being relatively consistent throughout the year after this time. The observed change from one mode of shoreline variability to another suggests that beaches can adapt relatively quickly to subtle changes in the intra-annual distribution of wave energy. Copyright © 2016 John Wiley & Sons, Ltd.

KEYWORDS: shoreline variability; storm frequency; shoreline forecasting; equilibrium shoreline modelling; Gold Coast, Australia

Introduction

Nearshore morphology along sandy coastlines has been recognized as a dynamic feature adjusting to changes in wave energy that subsequently influences the cross-shore movement of the shoreline (Wright and Short, 1984; Quartel, 2009; Price and Ruessink, 2013; van de Lageweg *et al.*, 2013). During periods of low wave energy, sand is observed to gradually move onshore and beaches accrete slowly with the creation of a berm. In contrast, higher energy wave events associated with the passage of storms lead to rapid erosion and the formation of sandbars in the surf zone (Shepard, 1950; Komar, 1976; Larson *et al.*, 1988). The balance of these constructive and destructive forces influence the overall stability of the beach.

The fact that beaches have persisted for thousands of years along sandy coastlines worldwide indicates that beaches can evolve and adapt to environmental changes that may span a broad range of temporal and spatial scales, including wave forcing and regional sediment supply. A clear example of this is provided in the seminal works of Wright and Short (1984) and Wright *et al.* (1985) that identify thresholds of morphological change based on the dimensionless sediment fall velocity parameter, Ω . The calculation of dimensionless fall velocity, Ω (Gourlay, 1968) is given by

$$\Omega = \frac{H_{sb}}{w_s T_p} \quad (1)$$

where H_{sb} is the breaking significant wave height (m), w_s is the sediment fall speed (m/s) and is generally assumed to be constant, and T_p is the spectral peak wave period (s).

At the lower wave energy end of the intermediate beach states ($1 < \Omega < 4$), sediment exchange between the nearshore and shoreline is typically observed to be rapid, responding at time-scales of days to weeks, corresponding to the passage of individual storms followed by post-storm beach recovery (Short and Hesp, 1982; Wright and Short, 1984; Splinter *et al.*, 2014a). In contrast, at highly dissipative beaches ($\Omega > 6$) exhibiting multiple sandbars and generally milder slopes, cross-shore sediment transport gradients are characteristically smaller and these beaches more commonly exhibit a seasonal variability (several months) in the shoreline position linked to underlying seasonal variation in wave climate (Wright and Short, 1984; Alexander and Holman, 2004; Splinter *et al.*, 2014a; Senechal *et al.*, 2015). The impact of seasonality (or changes thereof) of storms remains unclear as storm response is a function of present beach state as well as the individual storm conditions (Coco *et al.*, 2014).

This study is stimulated by an intriguing observation of the rather distinct change in the behavior of the shoreline at an open coast beach located along the east coast of Australia. As previously noted in Davidson and Turner (2009), following several years of the shoreline being observed to predominantly move cyclically landwards–seawards on an annual basis

corresponding to winter and summer periods, during 2005 there was an observed reduction in the seasonality of the waves and correspondingly the shoreline behavior. Extending here their original 6-year data set by an additional two years (2000–2008), it is further evident that post-2005 a predominantly storm-dominated mode of shoreline behavior had emerged. This apparent shift in the dominant mode of shoreline variability at this site provides the opportunity here to further explore the likely drivers and time-scales of sandy beach response and adjustment to changing wave conditions.

Ruessink *et al.* (2009) previously examined sandbar data at the Gold Coast to describe the short-term variability, inter-annual patterns and episodic sandbar migration events at this predominantly double-bar beach system. A distinctive seasonal variability with both bars moving offshore during the first half of the year and moving onshore during the latter half of the year was identified. However, super-imposed on this cyclic behavior and occurring during several episodic and high-energy storm wave events, the sandbars behaved in a very different manner. Both sandbars were observed to move offshore. Post-storm the outer bar moved onshore and disintegrated, with the inner bar shifting seawards to the initial position of the outer bar. However, this sequence of events was not observed if another large storm event occurred in close succession. A primary conclusion of this previous study was that the chronology and timing of storm events significantly determined the subsequent evolution of sandbar morphology. However, no analysis was undertaken of the main feature of the beach that is observed to vary at this site, namely the cross-shore movement of the shoreline.

In addition to new analyses of the shoreline and wave data spanning the period of a distinct change from seasonal to storm-dominated beach behavior, the use of a numerical shoreline model also provides a useful tool to explore more generically the rate at which beaches can potentially adjust to changing storminess. In the past decade a variety of equilibrium-based models have emerged to describe the observed association between wave forcing and beach response (Plant *et al.*, 1999, 2008; Miller and Dean, 2004; Davidson and Turner, 2009; Yates *et al.*, 2009; Splinter *et al.*, 2011, 2014a; Davidson *et al.*, 2013). Importantly, these models inherently assume a degree of stationarity over the time-scales of model application in order to produce reliable results in hindcasting (Splinter *et al.*, 2013a, b). By applying one such model separately to the combined, pre-, and post-time periods spanning the observed change of shoreline behavior at the Gold Coast during 2005, useful additional insight can be gained to the likely response of beaches to changing wave conditions.

The following section describes the available shoreline and wave data for this work and the simple equilibrium model that is used to further examine cross-shore processes related to the temporal variability in shoreline response to changing waves. The third section presents results pertaining to the analysis of the shoreline and waves, pre- and post-2005. These results are further discussed in the fourth section, with general conclusions presented in the final section.

Methods

Study site

The Gold Coast is located on the east coast of Australia (Figure 1). The 1 km long study site is a representative section of a 20 km long, straight stretch of coastline absent of headlands, with a median grain size (D_{50}) of 0.25 mm (Davidson *et al.*, 2013). The modal nearshore morphology is characterized by a double sandbar system (van Enckevort *et al.*, 2004; Ruessink

et al., 2009). The mean significant wave height (H_s) for the site is 1.14 m and the average peak wave period (T_p) is 9.4 s (refer to section 'Wave data' for further details). The modal wave direction is from the southeast, which results in a net northerly longshore transport estimated to be of the order of 0.5 M m³/yr. Alongshore gradients in longshore transport at the space- and time-scales examined in this study are not observed (Delft, 1970, 1992; Patterson, 2007; Splinter *et al.*, 2012) and are therefore not relevant to the shoreline behavior considered here.

Shoreline data

An ARGUS coastal imaging station (Holman *et al.*, 2003) comprising four cameras elevated 100 m above sea level and spanning a 180° field of view was operational at the study site between July 1999 and October 2008. This camera system provided hourly daylight images of the beach for shoreline mapping extending 5 km in the alongshore direction and 900 m cross-shore. To exclude any potential influence of prior nourishment works and the construction of an artificial reef down-drift of the study site in 1999 (Black and Mead, 2001; Turner, 2006), images obtained from mid-2000 onwards and located up-drift of the reef and nourishment were used in the present study. More specifically, the 1 km alongshore section of beach that is analyzed here is located 2 km up-drift of the reef and 1 km up-drift of the prior nourishment area. Previous work has shown this region of the beach to be well outside the influence of the down-drift engineering works (Turner, 2006).

Shoreline data were extracted from the ARGUS images using the Pixel intensity clustering (PIC) technique as described in Aarninkhof *et al.* (2003) and Plant *et al.* (2007). An additional criterion was applied such that images were used only when the significant wave height was less than 1 m, effectively limiting the potential landward bias of the mapped shoreline by wave setup and swash (refer to Davidson and Turner (2009) for further details). Briefly, the PIC technique is based on first transforming raw image intensities captured in their native Red-Green-Blue (RGB) color space to hue-saturation-value (HSV) color space, then using the resulting HSV values to separately and objectively cluster 'wet' and 'dry' pixels to delineate the shoreline. All shorelines used here were mapped at mid-tide and subsequently geo-rectified (Holland *et al.*, 1997) to a standard 5 m × 5 m grid resolution. The resolution of the rectified original images was approximately $dx < 4$ m (cross-shore) and $5 \text{ m} < dy < 20$ m (alongshore) for the study area used here. As detailed in Davidson and Turner (2009), horizontal uncertainty in the mapped shoreline position was +10.5 m and −5 m relative to the measured value. Weekly shorelines were extracted from the database and alongshore-averaged over the 1 km study area to effectively remove the influence of small-scale alongshore variability such as beach cusps and other smaller-scale localized shoreline perturbations. The shoreline time series was also filtered using a 6-week running mean to remove short (temporal) scale fluctuations. The full 8-year time series of shoreline data is shown in Figure 2.

Wave data

Hourly wave data (significant wave height H_s ; and peak wave period T_p) are available from an offshore wave rider buoy for the period 1995 to 2008 (95% recovery rate, outliers (defined by $T > 25$ s) and gaps were filled by linear interpolation). The wave rider buoy is located approximately 2 km to the east and 4 km north of the study site in 17 m water depth (Figure 1). For application of the shoreline model discussed below,

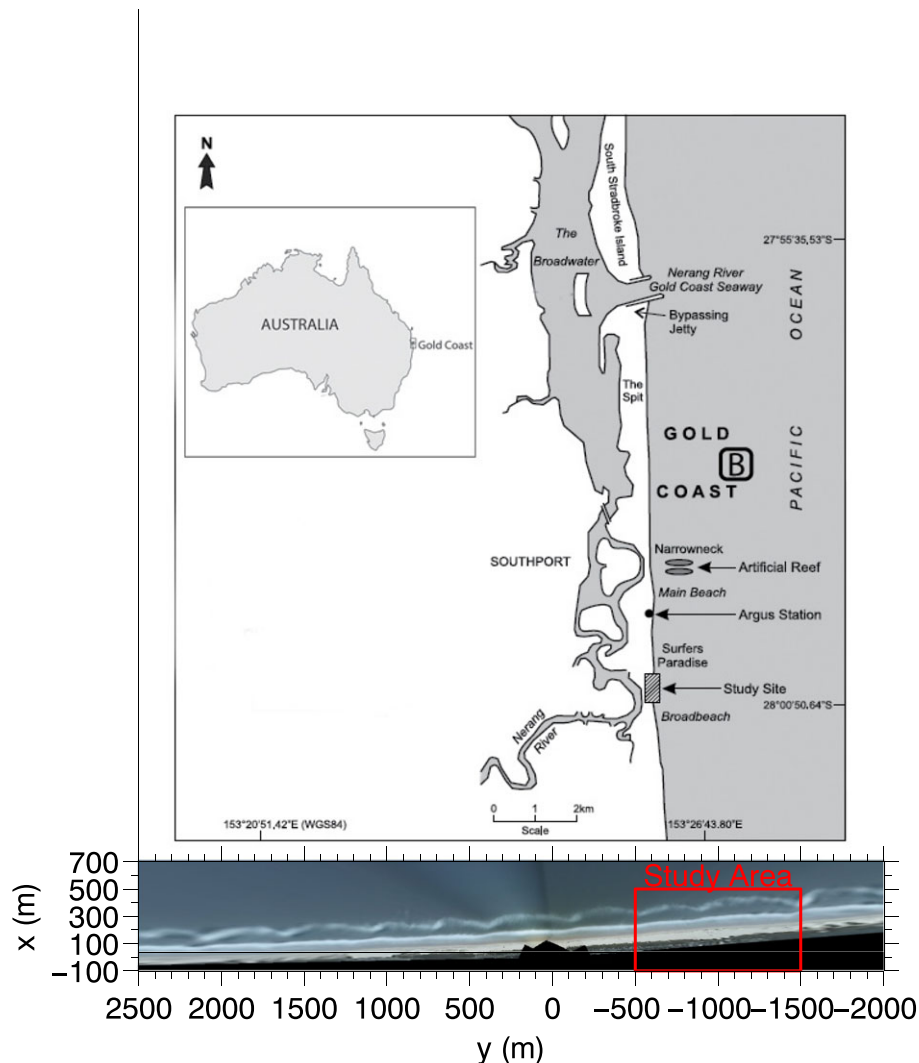


Figure 1. (top) Location map of Gold Coast, Australia showing study location. 'B' indicates location of the wave buoy in 17 m water depth. (bottom) Plan view Argus image with the study site highlighted. [Colour figure can be viewed at wileyonlinelibrary.com]

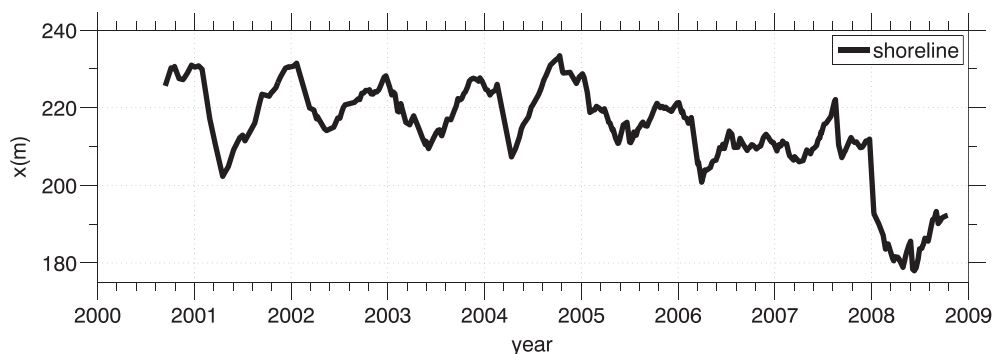


Figure 2. Time series of 1 km alongshore-averaged shoreline at Gold Coast, Australia. Shoreline have been filtered using a 6-week running mean.

corresponding breaking wave heights were estimated by shoaling the waves to the depth-limited breakpoint ($H_{sb}/h = \gamma = 0.78$, (McCowan, 1894)), where h is water depth and H_{sb} is the breaking (significant) wave height. Referring to the upper and middle panels of Figure 3, breaking wave heights are used in this study to quantify (by Equation (1)) the modal and time-varying dimensionless fall velocity at the site.

Characterizing the occurrence and duration of individual storms (upper panel Figure 3) follows the methodology proposed by Masselink *et al.* (2014). By this approach a storm

was defined to have occurred when two criteria were both met: (1) the breaking significant wave height, H_{sb} , exceeds $H_{95\%}$; and (2) $H_{sb} > H_{75\%}$ for a minimum 24 h. The start of the storm is thus defined when H_{sb} first exceeds $H_{75\%}$ and ends when H_{sb} drops below $H_{75\%}$. Further details of the magnitude and frequency of storm waves recorded at the Gold Coast are provided in the section 'Wave analysis'. Note that as to fully encapsulate the recorded storm characteristics at the Gold Coast study site, the entire wave record spanning 1995 to 2008 is examined.

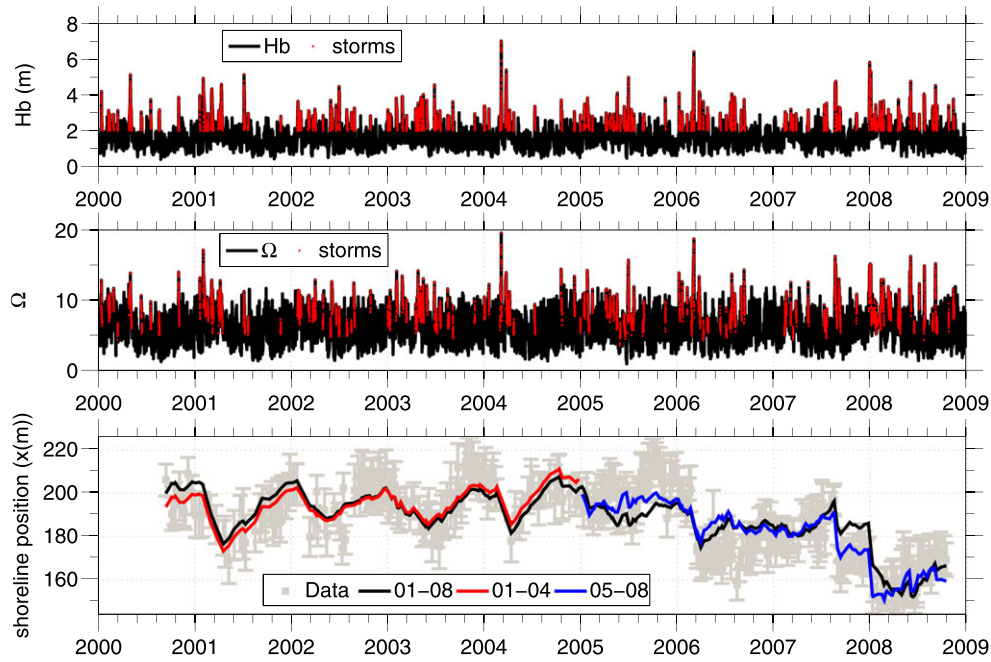


Figure 3. (top) Time series of breaking wave heights and (middle) dimensionless fall velocity with identified storms after Masselink *et al.* (2014) given in red. (bottom) *ShoreFor* results for calibration to the full time series for 2001–2008 (black); 2001–2004 (red); and 2005–2008 (blue). [Colour figure can be viewed at wileyonlinelibrary.com]

Overview of the *ShoreFor* equilibrium shoreline model

To provide an additional analysis tool to explore more generically the rate at which beaches and more specifically the shoreline can potentially adjust to changing storminess, the equilibrium-based *ShoreFor* model (Davidson *et al.*, 2013) was adopted. Importantly, previous applications of the model at a range of sites worldwide have demonstrated that, provided sufficient calibration data is available (Splinter *et al.*, 2013a), the model can successfully reproduce observed storm to seasonal cross-shore shoreline variability at a range of time-scales spanning from weeks up to a decade (Splinter *et al.*, 2014a).

Of particular relevance to this study, under-pinning the *ShoreFor* modelling approach is the concept that cross-shore sediment transport can be directly related to temporal variability in wave height and wave period (i.e. incident wave energy flux and dimensionless fall velocity). Briefly, the governing equation in *ShoreFor* that describes the cross-shore rate of shoreline change (dx/dt) is given by Davidson *et al.* (2013):

$$\frac{dx}{dt} = c(F^+ + rF^-) + b \quad (2)$$

where c ($\text{m}^{1.5} \text{s}^{-1} \text{W}^{-0.5}$) is referred to as the rate parameter; and F ($\text{W}^{0.5} \text{m}^{-0.5}$) is the forcing term, that in turn is split into two separate accretion (F^+) and erosion (F^-) components. The erosion component is multiplied by an erosion ratio (r), which accounts for the differing physical processes associated with accretion and erosion (for further discussion see Miller and Dean (2004); Yates *et al.* (2009); and Splinter *et al.* (2011)). The model also includes a simple linear term (b ; m/s) to acknowledge longer-term processes (typical time-scale of decades) that are not included in the wave-driven cross-shore sediment transport formulation, such as gradients in longshore transport, sediment sources/sinks and sea level rise. As was noted previously, alongshore gradients in longshore transport at the space- and time-scales examined in this study are not a feature at this study site, and is consistent with other recent work

(Ruggiero *et al.*, 2005; Harley *et al.*, 2011) that gradients in longshore transport are generally not expected to dominate the shorter-term (storm to seasonal) response along sandy coastlines.

Within the *ShoreFor* formulation summarized by Equation (2), the accretion/erosion forcing term, F , is defined as:

$$F = P^{0.5} \frac{\Delta\Omega}{\sigma_{\Delta\Omega}} \quad (3)$$

where $P = EC_g$ (W) is the breaking wave energy flux (with $E = \frac{1}{16}\rho g H_{sb}^2$ and $C_g = \sqrt{gh_b}$ and ρ = density of salt water (1025 kg m^{-3}); g = acceleration due to gravity (9.81 m s^{-2}); h_b = breaking wave depth); $\Delta\Omega$ is the disequilibrium in the dimensionless fall velocity between the instantaneous value and a time-averaged antecedent equilibrium condition; and $\sigma_{\Delta\Omega}$ is the standard deviation of $\Delta\Omega$. The disequilibrium term is normalized by $\sigma_{\Delta\Omega}$, so that the magnitude of response is governed by P , rather than $\Delta\Omega$. The erosion ratio (r) is numerically evaluated within the model to maintain the balance between accretion and erosion forcing such that no trend in the integrated values of F^+ and F^- results in no trend in the modelled shoreline:

$$r = \left| \frac{\sum_{i=0}^N \langle F_i^+ \rangle}{\sum_{i=0}^N \langle F_i^- \rangle} \right| \quad (4)$$

where $||$ indicates the absolute value, $\langle \rangle$ indicates a numerical operation that removes the linear trend but preserves the record mean, and N is the total record length.

The equilibrium condition in the model (Ω_{eq}) is time-varying and based on the weighted mean of past wave conditions, represented by the dimensionless fall velocity (Ω):

$$\Omega_{eq} = \left[\sum_{i=1}^{2\phi} 10^{-i/\phi} \right]^{-1} \sum_{i=1}^{2\phi} \Omega_i 10^{-i/\phi} \quad (5)$$

where i is the number of days before the present time and ϕ is the response factor (days).

Of particular relevance to this generic application of *ShoreFor* used here to explore the potential role of wave conditions in shifting the dominant mode of shoreline response from seasonal to a more storm dominated behavior, the model formulation includes the two wave dependent model parameters: c and ϕ . Optimization of the model based on a calibration to observed shoreline time series is achieved by first time-filtering the equilibrium response (Ω_{eq}) at pre-determined ϕ (response factor) values between 1 and 1000 days, as well as the time mean, and then solving for c as a function of ϕ . This enables optimization spanning the full 8 years of shoreline data (2000 to 2008) to be contrasted to separate model calibrations pre- and post-2005, and to use this approach to explore if any changes in the optimum value of ϕ are revealed by the model. As this response factor ϕ directly relates to the time period over which the 'best-fit' equilibrium frequency response of a monitored shoreline is determined, this approach is used below to examine and contrast the pattern of shoreline variability pre- and post-2005; and to then examine how this may relate to any change in the measured wave climate.

Results

It is useful to first define two time periods, denoted here as T1 and T2, differentiated by the observed change in shoreline behavior during 2005 that was originally identified in Davidson and Turner (2009). T1 encompasses shoreline position data from mid-2000 to the end of 2004 where a clearer annual signal in the shoreline is evident. The second time period (T2) spans the second half of the data set from 2005 to 2008, where a strong seasonal signal is not as evident and a storm-driven erosion and recovery signal emerges.

Shoreline analysis

To explore the observed change in shoreline behavior during 2005 that is evident in Figure 2, *ShoreFor* model coefficients optimized for different time periods are used here to provide further insight to the underlying time-scales at which the beach was observed to respond to continuously varying wave forcing.

A previous calibration of the *ShoreFor* model reported in Splinter *et al.* (2014a) for the full 8-year shoreline time series is reproduced in the lower panel of Figure 3. As noted earlier, shown in the upper and middle panels of this same figure are the corresponding time series of H_{sb} and Q with storms identified in red. The optimized response factor (ϕ), which is the key parameter of interest here as it defines the time period over which the equilibrium condition is calculated and is based on a 'best-fit' to the available wave and shoreline observations, was found to be 1000 days (95% skill interval is $650 \text{ days} \leq \phi \leq \text{time mean}$). This indicates that when the T1 and T2 time periods are combined, the dominant equilibrium response of the shoreline oscillated around the approximate time mean position. As the equilibrium condition is based only on past wave data, this long response time requires that the entire 1995 to 2008 wave data set that is available be used, so as to enable the slowly varying equilibrium shoreline position for the full 2000–2008 period to be calculated. Notably, despite the model being skillful when applied to the entire shoreline data set as shown in the lower panel of Figure 3 ($R^2 = 0.67$, $\text{NMSE} = 0.33$), it is observed that the magnitude of modelled response when calibrated to the full 8-year shoreline time series does not fully capture the large storm events in the latter half (2006 onwards) of the data set. Interestingly, a secondary band of skillful equilibrium

response existed between 50 and 130 days (peak skill at $\phi = 80$ days, $R^2 = 0.64$).

It is now useful to compare and contrast the above results with independent calibrations of the *ShoreFor* model to the separated time periods; T1 and T2, to determine if the two peaks in response factor found for the full calibration are temporally dependent. The results of these two separate calibrations are also shown in the lower panel of Figure 3. For T1 the calibration was found to be similar to the previously described full data set, with the optimized response factor (ϕ) again at 1000 days. The 95% skill interval was $500 \leq \phi \leq 1000$ days and no secondary peak in skill was observed. Note that, as the model utilizes 2ϕ days in the past to determine the time-evolving equilibrium condition (Equation (5)), wave data extending back to January 1995 were again required for this T1 model hindcast.

Significantly, when the model was calibrated to shoreline data from only the T2 period (2005–2008) the optimized response factor was now calculated to be an order of magnitude less ($\phi = 100$ days, 95% skill range $8 \leq \phi \leq 330$ days). This peak corresponds with the secondary peak found in the calibration to the full data set and confirms the temporal dependency of the response factor. This much-reduced response factor of the order of 100 days indicates a shoreline generally responding much more rapidly to shorter-term variability in wave conditions. Note that, because of the shorter optimum response factor for the time period T2 (i.e. $2\phi = 200$ days) wave data between mid-2004 and the end of 2008 were required. Table I summarizes the full and separate T1 and T2 optimized calibration coefficients and resulting model skill.

This application of the *ShoreFor* model that, at its core, is founded on the concept that cross-shore sediment transport at the shoreline can be directly related to temporal variability in wave height and wave period, reveals the rather striking (order of magnitude) difference in model response factor (ϕ) for the two time periods; T1 and T2. To investigate what the actual wave climate drivers were that underpin this apparent change in the dominant time-scale of shoreline response that was observed at the Gold Coast during 2005, more detailed analyses of the recorded wave climate are now presented.

Wave analysis

Mean wave conditions, total storm hours, storm intensity, storm duration, storm frequency and inter-storm recovery duration pre- and post-2005 were all quantified (note that the full wave record used for each of the two independent calibrations as described in the previous section were utilized). A two-sample student's t-test was used to test the statistical significance of any differences in wave climate characteristics between these two time periods. At the 95% significance level, this requires $P < 0.05$.

Average annual breaking wave heights were found to not change significantly ($P = 0.522$) between the two time periods. Up to the end of 2004, the mean annual breaking wave height was 1.69 m and after this was 1.72 m. This suggests that a simple change in mean wave height from T1 to T2 was probably not the driver of the observed (and modelled) change in shoreline behavior.

To test the hypothesis that changes in storm wave conditions were a key driver in the observed change in shoreline behavior, storm occurrence and duration (refer to section 'Wave data') were calculated. Spanning the full wave record period 1995–2008 the 95% exceedance breaking wave height ($H_{95\%}$) was 2.83 m and the 75% exceedance breaking wave height ($H_{75\%}$) was 2.0 m. Based on these criteria 183 individual storms were identified (upper and middle panel of Figure 3). Table II

Table I. Comparison of optimized *ShoreFor* calibration coefficients and resulting model skill (normalized mean square error (NMSE) and correlation (R)) for the three time periods of shoreline simulation: Full, T1 and T2

Time period	Φ (days)	C ($m^{1.5}s^{-1}W^{0.5}$)	Erosion ratio (r)	Linear rate (b, m/yr)	NMSE	R
Full (2001–2008)	1000	5.52e-8	0.45	−3.96	0.33	0.82
T1 (2001–2004)	1000	4.83e-8	0.48	2.77	0.45	0.74
T2 (2005–2008)	100	6.76e-8	0.46	−10.98	0.26	0.86

Table II. Average cumulative storm hours. Statistical significance was tested using a 2-sample student's *t*-test. The *P*-value indicates the probability of the means being equal

Time period	1995–2004 (T1) (h)	2005–2008 (T2) (h)	Δ (h)	<i>P</i> -value
Yearly	1111	1432	321	0.1733
Jan–June (JJ)	783	908	125	0.5155
July–Dec (JD)	395	638	243	0.0895
Δ (h)	388	270		
<i>P</i> -value	0.0049	0.2155		

summarizes the specific storm metrics and tests of significance discussed below.

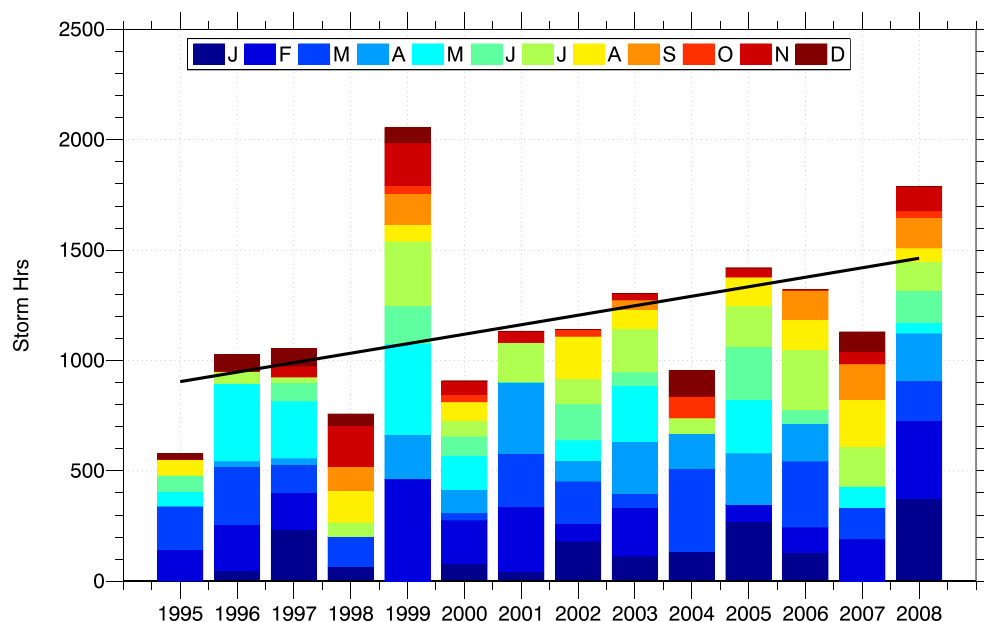
The total number of storm hours per year (separated by month) is presented in Figure 4. An increasing trend (43 h/yr, $R^2 = 0.217$, $P = 0.093$) in storm hours was observed between 1995 and 2008. Comparing the mean annual cumulative storm hours for the two time periods; T1 and T2, this was observed to increase by approximately 30% from 1111 h/yr to 1432 h/yr. However, this increase in mean annual cumulative storm hours is not statistically significant at the 95% level (Table II) due to the relatively large degree of inter-annual variability for the time period explored here (Figure 4). The general increase in cumulative storm hours per year spanning the full record length indicates either storms increased in duration or they increased in frequency, or both. Examining this further, the average length of an individual storm increased from 91 to 94 h between T1 and T2, indicating that individual storms only marginally increased in duration. A similar statistically insignificant ($P = 0.20$) increase in the average annual number of storms

observed (12 per year compared with 15 per year) was observed. In addition, the mean storm wave height ($P = 0.708$) and maximum storm wave height ($P = 0.450$) showed a statistically insignificant difference pre- and post-2005, indicating the overall intensity of storms did not vary.

The modest net increase over the total wave record length (1995–2008) in total storm hours revealed by Figure 4 can now potentially account for the emergence of a net erosion trend in the latter part of the shoreline record (refer to Figures 2 and 3). But it is not so readily apparent how this same increase in storm hours could have forced the distinctive and rather intriguing change in shoreline behavior that is visually evident in Figure 2 and further suggested by the results of the modelling in the section 'Shoreline analysis'.

The final aspect of a potential difference in wave forcing between the two time periods to be examined here is the intra-annual distribution of storms. Spectral analysis of the breaking wave height time series revealed that energy in the annual frequency band dropped by a factor of two post-2004. To test the hypothesis that this could be related to a shift in the temporal distribution of storms occurring each year, the wave data were further separated into two seasonal periods; the first half of the year from January to June (denoted JJ – summer/autumn), and the second half of the year from July to December (denoted JD – winter/spring).

The results of this analysis of intra-year storm occurrence reveals that pre-2005, a statistically significant difference ($P = 0.0049$) in the seasonal distribution of storm hours was present (JJ – 783 h compared with JD – 395 h). In addition, a statistically significant difference ($P = 0.0380$) in the mean recovery time between storms for the same period is also apparent (JJ – 24 days; JD – 58 days). This distinctive seasonality with

**Figure 4.** Cumulative storm hours by year. Each month is shown in a different color to highlight seasonality. A linear trend between 1995 and 2008 equal to 43 h/yr is plotted. R^2 (linear trend) = 0.217 ($P = 0.093$). [Colour figure can be viewed at wileyonlinelibrary.com]

nearly twice as many storm hours occurring in the first half of the year and associated halving of the available time for inter-storm recovery is consistent with the observed and modelled seasonal response in general shoreline behavior pre-2005. In contrast, for T2, the seasonal difference in total storm hours (JJ - 908 h; JD - 638 h) as well as the mean recovery time (JJ - 17 days; JD - 28 days) were not significant at the 95% level, indicating the seasonality in the storms had weakened from 2005 onwards. This marked change in the annual distribution of individual storm events, which is visible in Figure 5, now provides a plausible explanation for the change in shoreline behavior pre- and post-2005 that was observed at the Gold Coast.

Comparing the two time periods, the average annual total number of storm hours were greater for both the first half (JJ) and second half (JD) in T2, however, this increase is only significant for the latter (JD) period. A modest 15% increase in JJ total storm hours (T1=783 h; T2=908 h) is not statistically significant ($P=0.5155$) but would result in increased erosion. In contrast, storm hours for the latter half of each year (JD), where the beach typically recovered over a period of months, increased by >60% (T1=395 h; T2=638 h) and is statistically significant at the 90% level ($P=0.0895$). Mean recovery times did not significantly change (for JJ, $P=0.3106$; and JD, $P=0.2402$). This is further evidence that the seasonality of storms significantly decreased in the latter half of the data set, resulting in a more uniform distribution of larger wave energy events throughout the year and resulting decrease in the duration of the recovery time available between storms.

This changing intra-annual pattern of storms at the Gold Coast is explored further in Figure 5, which contrasts the average monthly distribution of total storm hours pre- and post-2005. Prior to 2005 (T1) the distribution is strongly skewed towards the first half of the year. The four summer and autumn months of February, March, April, May as well as July each recorded >100 storm hours per month on average. In contrast, post-2005 (T2) there is a clear spreading in this mean monthly distribution, with January through September (9 months) all exceeding on average 100 storm hours per month. In summary, commencing in 2005, the intra-annual pattern of wave forcing changed from a strongly seasonal signal to episodic storms becoming more evenly distributed throughout each year.

Discussion

An 8-year time series of weekly shoreline data collected at the Gold Coast, Australia, was used to examine the temporal evolution of a beach. Intriguingly, half way through the data set the movement of the shoreline at this site changed from a seasonally-dominated mode (annual cycle) to a storm-dominated (~monthly) mode and an erosive trend emerged. A shift in the observed beach cycle as described above has been related by previous researchers to the frequency and intensity of storms and inter-storm periods (Roberts *et al.*, 2013) which are further discussed below.

Seasonality in wave forcing

A statistically significant change in the annual average total storm hours (Figure 4) and more importantly the seasonal distribution of storms (Figure 5 and Table II) at the Gold Coast correlates well with the emergence of a net erosion trend in the latter half of the shoreline record and the observed disruption during 2005 of a seasonal erosion and accretion cycle of the shoreline. These observations agree with previous work whereby, the level of storminess, the frequency of storms/storm clusters, as well as the length of the storm season have all been shown to influence shorter-term (monthly to inter-annual) beach evolution (Fenster and Dolan, 1994; Coco *et al.*, 2014; Splinter *et al.*, 2014a, 2014b; Senechal *et al.*, 2015).

Pre-2005 at the Gold Coast there was a statistically significant difference in the total storm hours and recovery periods between the first and second half of the year. This seasonality corresponded to a general trend of a prolonged period of observed shoreline erosion (February–May), followed by a prolonged period of shoreline accretion (August–January), as has been observed elsewhere (Yates *et al.*, 2009; Splinter *et al.*, 2014a; Senechal *et al.*, 2015). Based on the first half of the shoreline data set presented here, the characteristic recovery time-scale of the Gold Coast beaches is on the order of several months.

In contrast, post-2005 it was found that on average 9 months each year (January–September) experienced more than 100 h

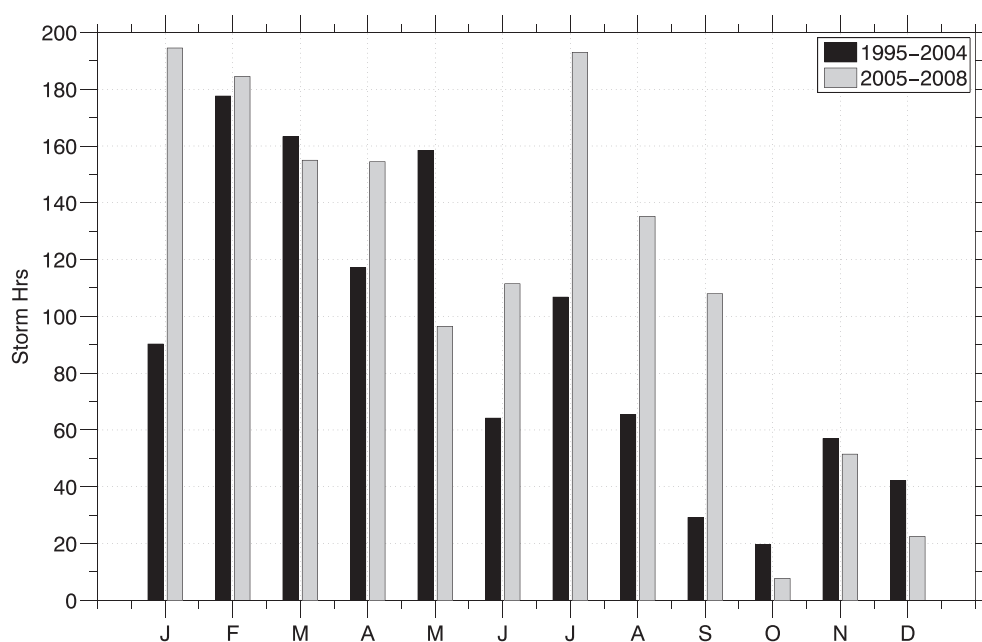


Figure 5. Comparison of average monthly distribution of storm hours for the two time periods pre and post the observed switch in shoreline behavior in January 2005.

of storm wave conditions per month (Figure 5), thus extending the erosion period and reducing the seasonality in the waves. Average recovery time post-2005 was less than 30 days. Comparing the two time periods, storm hours for the latter half of each year (July–December) increased by >60% pre/post 2005. Post-2005 it appears that erosion is accentuated due to storm frequency exceeding the time-scales of beach recovery (Morton *et al.*, 1995) and a temporal shift in the beach erosion/accretion cycle has occurred (Roberts *et al.*, 2013).

Shoreline and sandbar inter-dependency

While the simple equilibrium model used here attempts to encapsulate nearshore morphodynamics through the dimensionless fall velocity, Ω , (Wright and Short, 1984), the proximity and presence of sandbars at this double bar system probably also influences the temporal variability of the shoreline. Relating the shoreline and wave analysis presented above with previous work on sandbar morphodynamics at the Gold Coast (Castelle *et al.*, 2008; Ruessink *et al.*, 2009), further discussion of shoreline-sandbar inter-dependency is presented.

During storm events, sand is stripped from the shoreface and deposited in offshore sand bars. Both Castelle *et al.* (2008) and Ruessink *et al.* (2009) noted that following a large storm (for example, early 2006), the outer bar at the Gold Coast was located in deeper water and often decayed as it migrated back on shore. They observed that the decay and depth of the offshore bar offered reduced protection to the shoreline and inner bar (Price and Ruessink, 2011) for subsequent events and led to enhanced erosion of the shoreline as is seen in the latter half of the data presented in Figure 2.

Implications for modelling shoreline change

While a simple equilibrium shoreline model based on cross-shore processes was skillful at predicting the shoreline variability at this site (Figure 3), the optimized calibration parameters reveal two peaks in the underlying forcing response of the order 100 and 1000 days, respectively. This suggests that the beach exhibited 2 forcing-morphological coupling time-scales during the total monitoring period spanning 2000–2008. By separating the wave (forcing) and shoreline (response) calibration data into two separate time periods, corresponding to the observed change in shoreline behavior, repeating the model optimization process revealed that these peaks were in fact isolated to the two different time periods and did not occur simultaneously throughout the entire record (Table I). This temporal variability in optimized model coefficients has not previously been explored within the equilibrium model framework (Davidson and Turner, 2009; Yates *et al.*, 2009; Davidson *et al.*, 2013; Splinter *et al.*, 2014a).

The equilibrium model used here relates temporal changes in the forcing (waves) to changes in the observed shoreline time series. Based on the wave analysis presented here, the seasonality of storms (storminess) appears to influence the optimized filter value, Φ . Utilizing 13 data sets in their analyses, Splinter *et al.* (2014a) previously touched on this aspect when presenting parameterizations for their model coefficients based on mean wave conditions (Ω) as well as the relationship between the average storm (30 day, $\sigma_{\Omega 30}$) and annual (360 day, $\sigma_{\Omega 360}$) standard deviation in Ω . Conceptually, larger variability at the storm time-scale ($\sigma_{\Omega 30}$) would result in shorter Φ values for the same mean conditions. At the Gold Coast, post-2004 slight increases in mean Ω , $\sigma_{\Omega 30}$, and $\sigma_{\Omega 360}$ were observed. Based on Splinter *et al.* (2014a Figure 6), a decrease in Φ for T2 is not

expected, which is in contrast to the calibration results presented here. This would suggest that the relative importance of storminess and the seasonal distribution of storms, and perhaps sandbar–shoreline inter-dependency, is not accurately represented in the simple approach proposed by Splinter *et al.* (2014a) and requires further investigation.

Conclusions

Eight years of weekly shoreline observations at the Gold Coast revealed the intriguing observation that in 2005 the movement of the shoreline shifted from a seasonally-dominated mode (annual cycle) to a storm-dominated (~monthly) mode. Utilizing the calibration of an equilibrium shoreline model to explore the time-scales of underlying beach behavior, the hypothesis was tested that beaches can adapt relatively rapidly to a new modal state forced by quite subtle changes in the seasonality, intensity and storminess of the wave climate. More specifically, results presented suggest that a change in storminess and the temporal distribution of storms throughout the year can account for this observed change in the temporal variability of the alongshore-averaged shoreline. Analysis of the wave record showed that there was a shift in the seasonality of storm occurrence, from storms predominantly occurring in the first half of the year before 2005, to a more uniform annual distribution after this time. These observations suggest that when beaches are not given adequate time to recover between storms the cycle of beach erosion/recovery is interrupted, which can lead to enhanced erosion and vulnerability.

For the data set presented here, the general shoreline behavior responded rapidly (within a 12-month period) to the measured but relatively subtle change in wave conditions. Calibrating a simple equilibrium shoreline model to the two time periods pre and post revealed an order of magnitude difference in the best-fit frequency equilibrium response, suggesting a change in the underlying morphological adjustment of the beach to forcing conditions. This observation has potentially important and broader implications for the forecasting of future shoreline and morphodynamic response to changing regional wave climates worldwide. Our analysis suggest the need for a better understanding of the impact of not only storm intensity and changing wave conditions, but also storm frequency and shifting annual distribution, to the longer-term evolution of sandy coastlines in the coming decades.

Acknowledgments—Wave data was provided by Gold Coast City Council (<http://www.goldcoast.qld.gov.au/default.html>). ARGUS images from which shorelines and sandbar data were derived were provided by the Water Research Laboratory, UNSW Australia (<http://www.wrl.unsw.edu.au/>) with funding from Gold Coast City Council. The data for this paper are available by contacting the corresponding author. We thank the two anonymous reviewers and the Editors for their insightful comments that improved this manuscript. The authors have no conflict of interest to declare.

References

- Aarninkhof SGJ, Turner IL, Dronkers TDT, Caljouw M, Nipius L. 2003. A video technique for mapping intertidal beach bathymetry. *Coastal Engineering* **49**: 275–289.
- Alexander PS, Holman RA. 2004. Quantitative analysis of nearshore morphological variability based on video imaging. *Marine Geology* **208**(1): 101–111.
- Black K, Mead S. 2001. Design of the Gold Coast reef for surfing, beach amenity and surfing aspects. *Journal of Coastal Research, SI* **29**: 115–130.

- Castelle B, Corre Y, Tomlinson R. 2008. Can the gold coast beaches withstand extreme events? *Geo-Marine Letters* **28**(1): 23–30. DOI:10.1007/s00367-007-0086-y.
- Coco G, Senechal N, Rejas A, Bryan KR, Capo S, Parisot JP, Brown JA, MacMahan JHM. 2014. Beach response to a sequence of extreme storms. *Geomorphology* **204**: 493–501. DOI:10.1016/j.geomorph.2013.08.028.
- Davidson MA, Turner IL. 2009. A behavioral template beach profile model for predicting seasonal to interannual shoreline evolution. *Journal of Geophysical Research* **114**. DOI:10.1029/2007JF000888.F01020
- Davidson MA, Splinter KD, Turner IL. 2013. A simple equilibrium model for predicting shoreline change. *Coastal Engineering* **73**: 191–202. DOI:10.1016/j.coastaleng.2012.11.002.
- Delft. 1970. Gold Coast, Queensland, Australia - Coastal Erosion and Related Problems. Technical Report R257, Delft Hydraulics Laboratory, Delft, Netherlands.
- Delft. 1992. *Southern Gold Coast Littoral Sand Supply*. Technical Report H85, Delft Hydraulics Laboratory, Delft, Netherlands.
- Fenster MS, Dolan R. 1994. Large-scale reversals in shoreline trend along US mid-Atlantic coast. *Geology* **22**: 543–546.
- Gourlay MR. 1968. Beach and Dune Erosion Tests. Report M935/M936, Delft Hydraulics Laboratory, Delft, Netherlands.
- Harley MD, Turner IL, Short AD, Ranasinghe R. 2011. A re-evaluation of coastal embayment rotation: the dominance of cross-shore versus alongshore sediment transport processes, Collaroy-Narrabeen beach, SE Australia. *Journal of Geophysical Research* **116**: F04033. doi:10.1029/2011JF001989.
- Holland KT, Holman RA, Lippmann TC, Stanley J, Plant N. 1997. Practical use of video imagery in nearshore oceanographic field studies. *IEEE Journal of Oceanic Engineering* **22**(1): 81–92.
- Holman RA, Stanley J, Özkan-Haller HT. 2003. Applying video sensor networks to nearshore environmental monitoring. *IEEE Pervasive Computing* **2**(4): 14–21.
- Komar PD. 1976. *Beach Processes and Sedimentation*. Prentice-Hall, New Jersey.
- Larson M, Kraus NC, Sunamura T. 1988. Beach profile change: morphology, transport rate, and numerical simulation, in International Conference in Coastal Engineering, 1295–1309, Malaga, Spain.
- Masselink G, Austin M, Scott T, Poate T, Russell P. 2014. Role of wave forcing, storms and NAO in outer bar dynamics on a high-energy, macro-tidal beach. *Geomorphology* **226**: 76–93. DOI:10.1016/j.geomorph.2014.07.025.
- McCowan J. M.A D.Sc. 1894 XXXIX. On the highest wave of permanent type. *Philosophical Magazine Series 5* **38**(233): 351–358. DOI: 10.1080/14786449408620643.
- Miller JK, Dean RG. 2004. A simple new shoreline change model. *Coastal Engineering* **51**: 531–556.
- Morton RA, Gibeau JC, Paine JG. 1995. Mesoscale transfer of sand during and after storms; implications for prediction of shoreline movement. *Marine Geology* **126**: 161–179.
- Patterson DC. 2007. Sand Transport and Shoreline Evolution, Northern Gold Coast, Australia, in *Proceedings of the 9th International Coastal Symposium*, 147–151, *Journal of Coastal Research* SI 50.
- Plant NG, Holman RA, Freilich MH. 1999. A simple model for interannual sand bar behavior. *Journal of Geophysical Research* **104**(C7): 15755–15776.
- Plant NG, Aarninkhof SGJ, Turner IL, Kingston KS. 2007. The performance of shoreline detection models applied to video imagery. *Journal of Coastal Research* **23**: 658–670.
- Plant NG, Holland KT, Holman RA, Splinter KD, Reniers AJHM, Smit MWJ. 2008. A dynamical systems approach to analyzing morphodynamic states. In *River, Coastal and Estuarine Morphodynamics*; 217–221.
- Price TD, Ruessink BG. 2011. State dynamics of a double sandbar system. *Continental Shelf Research* **31**(6): 659–674. DOI:10.1016/j.csr.2010.12.018.
- Price TD, Ruessink BG. 2013. Observations and conceptual modeling of morphological coupling in a double sandbar system. *Earth Surface Processes and Landforms* **38**(5): 477–489. DOI:10.1002/esp.3293.
- Quartel S. 2009. Temporal and spatial behaviour of rip channels in a multiple-barred coastal system. *Earth Surface Processes and Landforms* **34**(2): 163–176. DOI:10.1002/esp.1685.
- Roberts TM, Wang P, Puleo JA. 2013. Storm-driven cyclic beach morphodynamics of a mixed sand and gravel beach along the Mid-Atlantic coast, USA. *Marine Geology* **346**: 403–421. DOI:10.1016/j.margeo.2013.08.001.
- Ruessink BG, Pape L, Turner IL. 2009. Daily to interannual cross-shore sandbar migration: observations from a multiple sandbar system. *Continental Shelf Research* **29**: 1663–1677.
- Ruggiero P, Kaminsky GA, Gelfenbaum G, Voigt B. 2005. Seasonal to interannual morphodynamics along a high-energy dissipative littoral cell. *Journal of Coastal Research* **21**: 553–578.
- Senechal N, Coco G, Castelle B, Mariu V. 2015. Storm impact on the seasonal shoreline dynamics of a meso- to macro-tidal open sandy beach (Biscarosse, France). *Geomorphology* **228**: 448–461. DOI:10.1016/j.geomorph.2014.09.025.
- Shepard FP. 1950. Beach cycles in southern California. Technical Report 20, USACE, Beach Erosion Board.
- Short AD, Hesp PA. 1982. Wave, beach and dune interactions in southeastern Australia. *Marine Geology* **48**: 259–284.
- Splinter KD, Holman R, Plant N. 2011. A behavior-oriented dynamic model for sand bar migration and 2DH evolution. *Journal of Geophysical Research* **116**. DOI:10.1029/2010JC006382.C01020
- Splinter KD, Davidson MA, Golshani A, Tomlinson RB. 2012. Climate controls on Longshore sediment transport. *Continental Shelf Research* **48**: 146–156. DOI:10.1016/j.csr.2012.07.018.
- Splinter KD, Turner IL, Davidson MA. 2013a. How much data is enough? The importance of morphological sampling interval and duration for calibration of empirical shoreline models. *Coastal Engineering* **77**: 14–27. DOI:10.1016/j.coastaleng.2013.02.009.
- Splinter KD, Davidson MA, Turner IL. 2013b. Monitoring data requirements for shoreline prediction: how much, how long, how often, in Proceedings of the 12th International Coastal Symposium (Plymouth England), *Journal of Coastal Research*, SI 65, ed by Conley DC, Masselink G, Russell PE, O'Hare TJ, 2179–2184.
- Splinter KD, Turner IL, Davidson MA, Barnard P, Castelle B, Oltman-shay J. 2014a. A generalized equilibrium model for predicting daily to interannual shoreline response. *Journal of Geophysical Research - Earth Surface* **119**: 1936–1958. DOI:10.1002/2014JF003106.
- Splinter KD, Carley JT, Golshani A, Tomlinson R. 2014b. A relationship to describe the cumulative impact of storm clusters on beach erosion. *Coastal Engineering* **83**(0): 49–55. DOI:10.1016/j.coastaleng.2013.10.001.
- Turner IL. 2006. Discriminating modes of shoreline response to offshore-detached structures. *Journal of Waterway, Port, Coastal, and Ocean Engineering* **132**: 180–191.
- van de Lageweg WI, Bryan KR, Coco G, Ruessink BG. 2013. Observations of shoreline-sandbar coupling on an embayed beach. *Marine Geology* **344**: 101–114. DOI:10.1016/j.margeo.2013.07.018.
- van Enckevort IMJ, Ruessink BG, Coco G, Suzuki K, Turner IL, Plant NG, Holman RA. 2004. Observations of nearshore crescentic sandbars. *Journal of Geophysical Research* **109**. DOI:10.1029/2003JC002214.C06028
- Wright LD, Short AD. 1984. Morphodynamic variability of surf zones and beaches: a synthesis. *Marine Geology* **56**: 93–118.
- Wright LD, Short AD, Green MO. 1985. Short-term changes in the morphodynamic states of beaches and surf zones: an empirical predictive model. *Marine Geology* **62**: 339–364.
- Yates ML, Guza RT, O'Reilly WC. 2009. Equilibrium shoreline response: observations and modeling. *Journal of Geophysical Research* **114**. DOI:10.1029/2009JC005359.C09014